Broadly reactive human monoclonal antibodies targeting the pneumococcal histidine triad protein protect against fatal pneumococcal infection

Short title: PhtD human antibodies

Jiachen Huang,[1,2] Aaron D. Gingerich,[1] Fredejah Royer,[1] Amy V. Paschall,[3,4] Alma Pena-Briseno,[1] Fikri Y. Avci,[3,4,] Jarrod J. Mousa[1,2,*]

[1]Center for Vaccines and Immunology, College of Veterinary Medicine, University of Georgia, Athens, GA, USA 30602

[2]Department of Infectious Diseases, College of Veterinary Medicine, University of Georgia, Athens, GA, USA 30602

[3]Department of Biochemistry and Molecular Biology, University of Georgia, Athens, GA 30602

[4]Center for Molecular Medicine, University of Georgia, Athens, GA 30602

*corresponding author: jarrod.mousa@uga.edu

Abstract

Streptococcus pneumoniae remains a leading cause of bacterial pneumonia despite the widespread use of vaccines. While vaccines are effective at reducing the incidence of most vaccine-included serotypes, a rise in infection due to non-vaccine serotypes, and moderate efficacy against some vaccine included serotypes have contributed to high disease incidence. Additionally, numerous isolates of *S. pneumoniae* are antibiotic or multi-drug resistant. Several conserved pneumococcal proteins prevalent in the majority of serotypes have been examined as vaccines in preclinical and clinical trials. An additional, yet unexplored tool for disease prevention and treatment is the use of human monoclonal antibodies (mAbs) targeting conserved pneumococcal proteins. Here, we isolate the first human mAbs (PhtD3, PhtD6, PhtD7, PhtD8, PspA16) against the pneumococcal histidine triad protein (PhtD), and the pneumococcal surface protein A (PspA), two conserved and protective antigens. mAbs to PhtD target diverse epitopes on PhtD, and mAb PspA16 targets the N-terminal segment of PspA. The PhtD-specific mAbs bind to multiple serotypes, while mAb PspA16 serotype breadth is limited. mAbs PhtD3 and PhtD8 prolong the survival of mice infected with pneumococcal serotype 3. Furthermore, mAb PhtD3 prolongs the survival of mice in intranasal and intravenous infection models with pneumococcal serotype 4, and in mice infected with pneumococcal serotype 3 when administered 24 hours after pneumococcal infection. All PhtD and PspA mAbs demonstrate opsonophagocytic activity, suggesting a potential mechanism of protection. Our results provide new human mAbs for pneumococcal disease prevention and treatment, and identify epitopes on PhtD and PspA recognized by human B cells.

Introduction

Streptococcus pneumoniae remains a leading cause of infectious morbidity and mortality despite the widespread use of two vaccines for disease prevention (1). The World Health Organization estimates over 1 million deaths occur worldwide each year due to pneumococcal infection (2). Similar to other respiratory pathogens, individuals below the age of 2 and above 65 years of age are more susceptible to invasive pneumococcal disease (3). In addition, there is also an increased frequency and risk of severe infection in individuals with preexisting conditions, including those with diabetes, chronic obstructive pulmonary disease, cardiovascular diseases, and human immunodeficiency virus (4). Although vaccination is widespread in the developed world, pneumococcal infection is responsible for 30% of adult pneumonia and has a mortality rate of 11-40% (5). Furthermore, in regions of the world with high childhood mortality rates, pneumococcal pneumonia is the cause of death for 20-50% of children (6).

S. pneumoniae is a common resident of the upper respiratory tract (7), and pneumococcal carriage precedes active infection (8). In young children, carriage rates of *S. pneumoniae* can be as high as 40-60% (9). Colonization is typically asymptomatic, however, *S. pneumoniae* can rapidly disseminate, often following a primary infection such as influenza (10) or COVID-19 (11), to cause pneumonia and invasive disease. Repeated colonization with *S. pneumoniae* typically results in immunization, and several studies have determined that colonization induces serum antibody responses to the capsular polysaccharide (12), and both serum antibody (13–17) and cellular immune responses to protein antigens (18, 19). These antibody levels in serum increase during the first few years of life (16), but tend to decrease in the elderly (20), which may contribute to the higher risk of disease in children and the elderly.

The majority of *S. pneumoniae* isolates are encapsulated, and 100 capsular serotypes have been identified (21), which are based on differences in the chemical structures of the capsular polysaccharide in each serotype (22). Current vaccines are based on eliciting opsonophagocytic antibody responses to the capsular polysaccharide, and utilize either a 13-

valent diphtheria toxoid conjugate vaccine to elicit T-dependent, high-affinity, and class-switched antibody responses (PCV13), or a 23-valent capsular polysaccharide mixture (PPSV23) to elicit T-independent antibody responses, or as a booster to PCV13. Anti-glycan antibodies produced in response to the vaccine are serotype-specific due to the distinct chemical structures of the capsular polysaccharides (23). Although vaccines have been highly effective at reducing the incidence of pneumococcal disease, a rise in the incidence of non-vaccine serotypes has occurred, termed serotype replacement (24). In addition, the incidence of invasive disease due to serotypes 3 and 19A have persisted in some reports despite widespread vaccination (25). In terms of treatment, antibiotic resistance among non-vaccine serotypes has risen, and presents challenges in treating pneumococcal infection (26). Based on the limitations of current vaccines and treatments, additional options are currently being explored. For many years, such research has focused on developing vaccines that are broadly reactive, primarily based on the idea that conserved protein antigens present in the majority of pneumococcal serotypes would be effective at preventing disease independent of serotype (27). Multiple antigens have been tested in preclinical infection models, with several entering clinical trials, including the toxin pneumolysin, pneumococcal surface protein A (PspA), pneumococcal surface antigen A (PsaA), pneumococcal choline binding protein A (PcpA), PcsB, serine threonine kinase protein (StkP), and pneumococcal histidine triad protein (PhtD) (28).

PhtD is a member of a group of conserved surface proteins on *S. pneumoniae* that also includes PhtA, PhtB, and PhtC, all of which share histidine triad motifs (29). The proteins have high sequence homology to each other, and PhtB and PhtD share 87% sequence homology (30). PhtD is highly conserved, varying 91-98% among strains isolated from invasive disease cases in children (31). One study of 107 pneumococcal strains showed PhtD was expressed in 100% of tested serotypes (30), while other studies have found PhtD is widely prevalent but is absent in a subset of isolated strains (32–34). The function of the Pht family of proteins has not been fully elucidated, although data has implicated the proteins in attachment of *S. pneumoniae*

to respiratory epithelial cells (35, 36). In addition, the first histidine triad motif of PhtD has been shown to be important for zinc acquisition and bacterial homeostasis (37). Although the full structure of PhtD has not been determined, a crystal structure of the third histidine triad motif bound to Zn^{2+}, and a solution NMR structure of the N-terminal fragment of PhtD has been determined (38, 39). All Pht proteins are immunogenic and induce protective humoral immunity, and vaccination with these proteins was shown to reduce colonization, sepsis, and pneumonia (29, 40, 41). PhtD has been shown to protect against systemic pneumococcal disease in a mouse model (29), and immunization of rhesus macaques with PhtD along with detoxified pneumolysin protected the animals against pneumococcal infection (42). Fragments of PhtD have also been assessed for protective efficacy, and somewhat conflicting reports have demonstrated that both the N and C terminus are immunogenic and protective (43, 44). PhtD was recently used as an antigen in a phase IIb clinical trial, demonstrating that PhtD remains an antigen of interest in pneumococcal vaccinology, although PhtD was administered along with PCV13, so a direct comparison of PhtD vs PCV13 was not accomplished (45). Mouse monoclonal antibodies to PhtD were shown to protect mice using a macrophage and complement dependent mechanism (46), and human polyclonal antibodies to PhtD were shown to reduce adherence of the pneumococcus to lung epithelial cells and reduce murine nasopharyngeal colonization (47). Human polyclonal antibodies generated in response to alum adjuvanted PhtD vaccination were also shown to protect mice from pneumococcal disease (48).

Another vaccine antigen, PspA, is an important virulence factor of *S. pneumoniae* and one of the most abundant surface proteins (49). As with PhtD, PspA is found in the majority of examined clinical isolates (33, 50). PspA mutant strains are cleared faster from the blood of mice compared to intact strains (51), and vaccination with PspA protects mice from pneumococcal infection (52–58). PspA is less conserved than PhtD, and is grouped into three families with >55% identity, and six clades with >75% identity (59). PspA has four distinct structural domains, including the alpha-helical region, the proline rich region, the choline binding

repeat domain, and the cytoplasmic tail, of which the proline rich region is highly conserved across clades, while the N-terminal alpha-helical region is more variable (60). PspA has been shown to inhibit complement deposition (61–63), and has shown specificity for binding of human lactoferrin, although the importance of this binding is unclear (64). An X-ray crystal structure of the lactoferrin binding domain of PspA in complex with the N-terminal region of human lactoferrin has been determined (65). Mouse mAbs to PspA have been shown to prolong survival of mice, and improve efficacy of antibiotic treatment (64). Additionally, antibodies isolated from humans following immunization with recombinant PspA are broadly cross-reactive and protect mice from pneumococcal infection with heterologous PspA (66, 67). A clinical trial of a recombinant attenuated salmonella typhi vaccine vector producing PspA has been completed (NCT01033409), and a protein-based Phase Ia clinical trial incorporating PspA is current underway (NCT04087460).

It is well-defined that antibodies can prevent pneumococcal infection based on the success of antibody-based pneumococcal vaccines. Since both PspA and PhtD are protective antigens, and elicit protective antibodies, it is reasonable to assume that human mAbs to these antigens would be protective. As these proteins are highly conserved across pneumococcal serotypes, mAbs to PhtD and PspA could prevent and possibly treat disease from a broad-spectrum of pneumococcal serotypes. Human mAbs are promising as therapeutics for bacterial pathogens, as bezlotoxumab was FDA approved for prevention of recurrent *Clostridium difficile* infection (68). However, there have been no human mAbs isolated to any pneumococcal protein antigens. Serum antibodies to PhtD and PspA are elicited in response to pneumococcal carriage (16, 69, 70), and in this study, we generated human monoclonal antibodies to PhtD and PspA from healthy human subjects. We determined the serotype breadth and epitope specificity of the mAbs, and demonstrated the protective efficacy of PhtD-specific human mAb in multiple mouse models of pneumococcal infection.

Results

Isolation of pneumococcal protein-specific human mAbs

To identify PhtD and PspA-specific human mAbs, we recombinantly expressed His-tagged PhtD and PspA from strain TCH8431 (serotype 19A) in *E. coli* **(Figure 1A)**, and utilized these proteins to screen stimulated B cells from human donor peripheral blood mononuclear cells (PBMCs) as previously described (71). PBMCs from healthy human subjects were plated onto a feeder layer expressing human CD40L, human IL-21, and human BAFF for six days to stimulate B cell growth and antibody secretion. Cell supernatants from the stimulated B cells were screened against recombinant PhtD and PspA by enzyme-linked immunosorbent assay. Responses to the recombinant proteins were varied between subjects as shown in an example in **Figure 1B**. From five subject PBMCs, we fused several reactive wells for generation of human hybridomas and subsequent human mAb isolation. Four hybridomas lines, each from unique donors, were successfully generated and biologically cloned by single cell sorting for PhtD, and one mAb was generated for PspA from an independent subject. Each of the mAbs to PhtD had similar binding EC_{50} values determined by ELISA **(Figure 1C)**, and mAbs to PhtD and PspA bound with high avidity with EC_{50} values ranging from 26-45 ng/mL **(Figure 1C, 1D)**. To determine the V, D, and J genes utilized by each mAb, the hybridomas were sequenced by RT-PCR followed by TA cloning and the results are shown in **Table 1**, and the sequences are provided in supplemental material. mAbs PhtD3 and PhtD6 utilize kappa light chains, while mAbs PhtD7 and PhtD8 use lambda light chains. All mAbs were of the IgG_1 isotype based on isotyping data determined by ELISA. All mAbs utilize unique heavy chain and light chain V genes, with the exception of mAbs PhtD7 and PhtD8, as these share predicted V_L and J_L gene usage, although LCDR3 sequences share little sequence identity. mAbs PhtD7 and PhtD8 share V_H and J_H gene usage, although vary in the use of the D_H gene, which leads to stark differences in CDR3 lengths, with mAbs PhtD7 and PhtD8 having 20 amino acid and 8 amino

172 acid length HCDR3 lengths, respectively. mAb PspA16 shares V gene usage with mAbs PhtD7
173 and PhtD8.
174
175 Epitope mapping of the human mAbs
176 To identify the specific regions of PhtD targeted by the human mAbs, we generated
177 truncated fragments of PhtD based on a secondary structure predictor. The fragments were
178 fused to the maltose binding protein (MBP) to ensure solubility, and expressed in *E. coli* and
179 purified using amylose resin. The majority of the fragments were >90% pure with the exception
180 of free MBP protein for the MBP fusion proteins **(Figure 2A)**. To identify the specific regions of
181 PhtD targeted by the isolated mAbs, we measured ELISA binding of mAbs to fragments of
182 PhtD. Since there are no previous mAbs that have been generated to these proteins with
183 defined epitopes, the generated fragments provide rough estimates of mAb epitopes. Each of
184 the four mAbs bind to a unique region on the PhtD protein **(Figure 2B)**. mAbs PhtD3 and PhtD6
185 bind the N-terminal portion of the protein, while mAb PhtD8 binds the C-terminal portion. mAb
186 PhtD7 appears to target a unique conformational epitope that is dependent on amino acids 341-
187 838, but this mAb does not bind 341-647 or 645-838 fragments. We next assessed the epitopes
188 of the mAbs by competitive biolayer interferometry to compare the binding epitopes between
189 mAbs. Anti penta-His biosensors were loaded with His-tagged PhtD protein, and mAbs were
190 competed for binding sequentially **(Figure 2C,2D)**. The mAbs bind distinct regions with limited
191 competition similar to results from the fragment ELISA data. mAbs PhtD3 and PhtD6 show
192 intermediate competition, and the epitopes for these mAbs also overlap in our fragment ELISA
193 data. To map the binding region of mAb PspA16, we fragmented PspA into several truncations
194 based on previously determined domains **(Figure 3A)** (60). mAb PspA16 had high avidity to
195 recombinant PspA, and bound to the N-terminal fragment 1-247 based on positive binding to
196 amino acid fragments 1-438 and 1-512 and negative binding to 247-512, 436-725, and 247-725
197 fragments **(Figure 3B)**.

198

199 Serotype breadth of the isolated PhtD-specific mAbs

200 Pneumococcal surface proteins PhtD and PspA are conserved across serotypes, and
201 are widely prevalent in the majority of serotypes. As such, human mAbs to these antigens could
202 have the potential to treat pneumococcal infection from multiple serotypes. In order to determine
203 the serotype breadth of the isolated mAbs, we initially assessed mAb binding to two diverse
204 pneumococcal serotypes, strain TCH8431 (serotype 19A), from which the genes for
205 recombinant PhtD and PspA proteins were cloned and expressed, and the commonly used
206 laboratory strain TIGR4 (serotype 4). PspA shares 88% amino acid sequence identity between
207 TCH8431 and TIGR4, although significant variability is present in the N-terminal domain, with
208 70% identity in amino acids 1-247. In contrast, PhtD shares 98% amino acid sequence identity
209 between these two strains. We conducted western blots by probing bacterial lysates from
210 TIGR4 and TCH8431 with mAbs PhtD3 and PspA16. mAb PspA16 only labels PspA protein
211 from strain TCH8431 **(Figure 4A)**, while mAb PhtD3 is able to label PhtD protein from both
212 pneumococcal strains. However, as the bacterial lysis likely results in protein denaturation, it is
213 possible the epitope for mAb PspA16 is altered during denaturation. We next determined if
214 mAbs isolated against each of the recombinant proteins bind whole bacteria. We conducted
215 ELISA assays by coating plates with fixed bacteria and measuring mAb binding by ELISA.
216 mAbs PhtD3, PhtD6, PhtD7, and PhtD8 were broadly reactive across multiple unrelated
217 pneumococcal serotypes, and mAbs PhtD3, PhtD6, and PhtD7 had higher avidity to fixed
218 bacteria as compared to PhtD8 **(Figure 4B)**. In contrast, PspA16 bound only to strain TCH8431,
219 similar to results from the western blot experiments. Since PspA16 binds to the most variable
220 region of PspA, the reduced binding to divergent serotypes was expected. In a third experiment,
221 we assessed binding of the mAbs to a panel of pneumococcal serotypes by flow cytometry. As
222 shown in **Figure 4C**, we utilized serum from a donor vaccinated 21 days previously with
223 Prevnar-13 as a positive control. The PhtD mAbs bound to the majority of tested serotypes, with

mAbs PhtD3 and PhtD8 showing the broadest binding. In contrast, PspA16 bound only to TCH8431 and the serotype 3 strain WU2.

PhtD3 protects mice from fatal pneumococcal infection

As mAbs PhtD3 and PhtD8 exhibited the highest overall breadth in the serotype binding analysis by flow cytometry, these mAbs were further analyzed for protective efficacy in the mouse model. In addition, these mAbs were chosen in order to identify if the epitope specificity of mAbs to PhtD affect protective efficacy, as they target nonoverlapping epitopes. Mouse mAbs to PhtD (46) and polyclonal human antibodies from both healthy human subjects (47) and PhtD-vaccinated humans (48) have been shown to protect against colonization or disease in mouse models of pneumococcal infection. However, no human mAbs have been examined for protective efficacy. To determine if the PhtD-specific mAbs protect against infection, we examined the efficacy of mAbs PhtD3 and PhtD8 in a mouse model of pneumococcal pneumonia with a serotype 3 strain (WU2), as serotype 3 is a leading cause of invasive pneumococcal disease (72). Since the mAbs were isolated from human hybridomas, and thus have authentic human Fc regions, we isotype-switched the Fc region to the closest mouse homolog (human IgG_1 became mouse IgG_{2a}). mAbs PhtD3 and PhtD8 chimeras with mouse IgG_{2a} Fc regions (PhtD3-IgG_{2a} and PhtD8-IgG_{2a}) were recombinantly expressed in HEK293F cells for testing in the mouse model. As a control for the study, we purchased a mouse IgG_{2a} isotype control antibody. We first examined the binding of the mAbs to ensure binding was still observed for the recombinant PhtD3-IgG_{2a} and PhtD8-IgG_{2a} mAbs, and that no binding was observed for the isotype control mAb. As expected, PhtD3-IgG_{2a} and PhtD8-IgG_{2a} had similar binding avidity to recombinant PhtD as hybridoma-derived PhtD, while the isotype control showed no binding **(Figure 5A)**. We first tested the prophylactic efficacy of PhtD3-IgG_{2a} and PhtD8-IgG_{2a} in a pneumonia model with pneumococcal serotype 3. Both mAbs prolonged the survival of mice compared to the isotype control, although those mice treated with mAb PhtD3

demonstrated higher survival (80% versus 30%) **(Figure 5B, 5C).** As mAb PhtD3-IgG_{2a} protected a larger percentage of mice, we chose this mAb for further analysis. mAb PhtD3-IgG_{2a} was then tested for protective efficacy against pneumococcal serotype 4 (TIGR4) to identify if the broad binding correlates to broad protection. In experiments with TIGR4, we used only an isotype control mAb group since no significant difference was observed between the PBS and isotype control mAb groups in the serotype 3 experiments. For this serotype, we used CBA/N mice for the intranasal infection model as TIGR4 was not sufficiently lethal by intranasal infection in C57BL/6 mice. CBA/N mice have previously been shown to be susceptible to serotype 4 (73). PhtD3-IgG_{2a} prolonged survival of mice, providing 93% protection compared to 47% for the isotype control **(Figure 5C)**. As we were not able to test PhtD3-IgG_{2a} in an intranasal infection model with TIGR4 in C57BL/6 mice, we conducted an experiment in C57BL/6 mice in which mice were intravenously infected with TIGR4 to model septic pneumococcal infection. In this study, PhtD3-IgG_{2a} prolonged survival of mice with 69% efficacy compared to 27% survival with the isotype control **(Figure 5D)**. The most clinically relevant scenario for mAb treatment of pneumococcal infection would be administration after pneumococcal infection. To model such a scenario, we infected mice with pneumococcal serotype 3, and administered mAb PhtD3-IgG_{2a} 24 hrs after infection. In this model, 65% of PhtD3-IgG_{2a} treated mice survived the infection compared to 10% for the isotype control group **(Figure 5E).**

<u>PhtD-specific human mAbs have opsonophagocytic activity</u>

The correlate of protection for current pneumococcal vaccines is based on the elicitation of anti-capsule antibodies that opsonize bacteria, leading to their phagocytosis by host immune cells and subsequent bacterial killing (74, 75). Mouse mAbs isolated by vaccination with PhtD were previously shown to induce bacterial opsonophagocytosis, which was dependent on complement and macrophages (46). To determine a potential mechanism of protection by

PhtD3, and additional PhtD mAbs, we utilized established opsonophagocytosis killing assays (OPKAs) using the HL-60 cell line. We tested the mAbs against serotypes 4 (strain TIGR4), 3 (strain WU2), and serotype 19A (strain TCH8431), from which our PhtD and PspA constructs were cloned. These mAbs were also compared to purified IgG obtained from a human subject previously vaccinated with Prevnar-13 21 days before blood collection, as the OPKA assay is the standard to measure vaccine uptake (76). All PhtD mAbs induced decreased colony forming units against all three serotypes compared to no antibody and an irrelevant mAb to human metapneumovirus **(Figure 6A)**. PspA16 also decreased colony forming units against all three serotypes, although the efficacy against serotype 4 was lower as expected based on the serotype binding data. To confirm these findings, we adopted a flow-based assay previously shown to work for group B Streptococcus (77). HL-60 cells were incubated with opsonized bacteria that were labeled with pHRodo, which leads to fluorescent HL-60 cells upon phagocytosis of labeled bacteria. Similar to our results from the OPKA assay, all PhtD mAbs induced an increase in pHRodo+ HL-60 cells compared to no antibody and isotype control antibody analyses **(Figure 6B)**. Purified IgG from an unvaccinated donor showed the highest number of pHRodo+ cells, as human IgG contains antibodies to multiple pneumococcal surface proteins. Interestingly, PspA16 also induced increased uptake to all three serotypes in this assay, although the highest activity was observed for serotype 19A, the serotype from which we cloned our PspA gene.

Discussion

In this study, we have isolated and determined the binding affinity, epitope specificity, serotype breadth, and protective properties of the first human mAbs to any pneumococcal surface protein. Both PhtD and PspA have been examined in depth as vaccine candidates for prevention of pneumococcal infection, although the current outlook for progress of these antigens in the era of conjugate vaccines remains uncertain. However, human mAbs to these conserved antigens offer the ability for pan-serotype recognition and potentially disease prevention and treatment. In contrast, human mAbs isolated following vaccination with pneumococcal polysaccharide vaccines are highly serotype specific (23), and would offer limited use in the clinic due to their highly specific serotype specificity.

Based on the B cell stimulation and screening results, it is clear that healthy individuals have circulating B cells specific to pneumococcal antigens PhtD and PspA. One drawback of our study is the lack of knowledge on the infection history of the human subjects used in the study. It has been previously shown that colonization by *S. pneumoniae* results in immunization, and it is unknown whether all of these donors were previously infected with *S. pneumoniae*. Therefore, the mAbs isolated here are likely the result of pneumococcal colonization, which resulted in class switched B cells with 85-94% somatic mutation, which is similar to previous work in our lab studying healthy individuals who were presumed to be previously infected with human metapneumovirus (71, 78). Each of the PhtD-specific mAbs was isolated from unique human subjects, and mAbs PhtD3, PhtD6, and PhtD7/8 utilized different heavy and light chain V genes. Interestingly, mAbs PhtD7 and PhtD8 utilize the same V gene in both heavy and light chain, yet differ in the predicted heavy chain J gene, which leads to highly different CDR3 lengths. Although these two mAbs share common heavy and light chain V genes, the epitopes for these mAbs do not compete and have only partial overlap based on the binding experiments with truncated protein fragments. It is a striking observation that the N-terminal specificity of mAbs PhtD3 and PhtD6 correlates with higher binding to whole cell bacteria compared to

PhtD8, as the N-terminal region of the protein is predicted to be attached to the bacterial surface, leaving the C-terminal half more surface exposed (35). Further mapping experiments through X-ray crystallographic analysis will help clarify this observation. Previous work has identified specific linear peptide epitopes that are immunodominant in pediatric patients with invasive pneumococcal disease, and these included AA 88-107, AA 172-191, and AA 200-219 (79). These peptides overlap with the epitopes for mAbs PhtD3 and PhtD6, although we have not yet determined if these mAbs bind these peptide epitopes. Overall, these data suggest the human antibody response to PhtD targets multiple epitopes. For PspA16, the mAb targets the N-terminal region of PspA, which has a high number of negatively charged residues, and has been shown to be protective in several studies (80). Mouse mAbs isolated against PspA were determined to target the N-terminal fragment as well, suggesting this domain is immunogenic in both mice and humans (80, 81). Although mAb PspA16 has limited serotype breadth, it is unclear if other human mAbs to PspA, even those targeting the N-terminal fragment, will be more broadly reactive. It is well established that the N-terminal region of PspA is more variable compared to the proline-rich region, and further studies will determine whether other PspA mAbs are more broadly-reactive than PspA16, as mAb PspA16 binds outside the highly conserved proline-rich region (82). Limitations of this current study include the limited number of mAb isolated for PhtD and PspA. Further isolation of mAbs will identify if the epitopes and gene usage of the mAbs described here are common in multiple donors.

Anti-pneumococcal mAbs have potential for use in the clinic, as current vaccines cover only a subset of current serotypes (although the most prevalent in invasive disease), and a rise in non-vaccine serotypes has occurred following vaccine introduction (24, 83). The prophylactic efficacy of mAbs PhtD3 and PhtD8 were demonstrated against pneumococcal serotype 3, a leading cause of invasive pneumococcal disease (24). We have also assessed the prophylactic efficacy of mAb PhtD3 against serotype 4 in both intranasal and intravenous infection studies, to model pneumococcal pneumonia and sepsis. Furthermore, we have demonstrated the mAb

PhtD3 prolongs survival of mice treated with the mAb 24 hrs after infection with pneumococcal serotype 3. As mAbs PhtD3 and PhtD8 target unique epitopes on the N-terminal and C-terminal region of PhtD, respectively, the higher survival of mAb PhtD3-treated mice suggests a potential role of epitope specificity in protective efficacy, although other factors such as functional activity, decreased binding to serotype 3 bacteria in the ELISA and flow binding assays compared to mAb PhtD3, CDR length and percent somatic hypermutation, and corresponding binding modes may be important for the observed differences. Further studies will need to be completed to determine the efficacy of other PhtD mAbs, to examine whether the specific epitope on PhtD indeed influences the protective efficacy of these mAbs, and to determine whether the mAbs protect against infection with additional serotypes. In addition, the delivery timing of the mAbs for optimal protection, the potential use of mAbs in combinations for improved protective efficacy, and the use of mAbs in concert with antibiotic treatment will need to be examined. Furthermore, as secondary pneumococcal infection is prominent following influenza (10) and SARS-CoV-2 infection (11), another potentially useful scenario for use of anti-pneumococcal mAbs would be administration following primary viral infection, to prevent secondary pneumococcal infection. Further studies will need to be completed to determine if mAb PhtD3 or other mAbs will protect against secondary infection.

A potential mechanism of protection for mAbs PhtD3 and PhtD8, and the functional activity of the other PhtD- and PspA-specific mAbs were assessed in opsonophagocytic assays. While showing activity in these *in vitro* assays, the mechanism of protection *in vivo* was not determined and will need to be further explored. mAbs to the pneumococcal capsular polysaccharide have been shown to be protective through multiple mechanisms, with even non-opsonic mAbs demonstrating protective efficacy and the ability to reduce pneumococcal colonization (84, 85). PhtD has been shown to be important for pneumococcal adherence (36, 86), and mAbs to PhtD have also been shown to limit adherence of bacteria (47). Therefore,

374 additional protective mechanisms for anti-PhtD mAbs exist and may work in concert with
375 opsonophagocytosis.

376 Overall, our study furthers the premise of using human mAbs to highly conserved
377 surface antigens for prevention and treatment of pneumococcal infection. In addition, the
378 application of human mAbs for other bacterial infections, particularly those that have concerns
379 of antibiotic resistance is an important path forward for the development of new therapies.
380 Further defining the epitope specificity of protective human mAbs to conserved pneumococcal
381 surface proteins would also facilitate the development of an epitope-based, and potentially
382 multi-antigen and broadly protective pneumococcal vaccine.

383

384

Material and methods

Ethics statement

This study was approved by the University of Georgia Institutional Review Board as STUDY00005127 and STUDY00005368. Healthy human donors were recruited to the University of Georgia Clinical and Translational Research Unit and written informed consent was obtained. For the Prevnar-13 vaccinated human samples, healthy subjects were recruited for vaccination with Prevnar-13, and a single blood sample was collected 21-28 days following immunization. All animal studies performed were in accordance with protocols approved by the Institutional Animal Care and Use Committee of the University of Georgia.

Blood draws and isolation of PBMCs

After obtaining informed consent, 90 mL of blood was drawn by venipuncture into 9 heparin-coated tubes, and 10 mL of blood was collected into a serum separator tube. Peripheral blood mononuclear cells (PBMCs) were isolated from human donor blood samples using Ficoll-Histopaque density gradient centrifugation, and PBMCs were frozen in the liquid nitrogen vapor phase until further use.

Pneumococcal protein cloning and expression

PspA and PhtD full-length proteins and fragments were cloned from the genome of *S. pneumoniae* strain TCH8431 (serotype 19A) with primers listed in **Table 2** below. The full-length PspA and PhtD were ligated into the pET28a vector while the fragments were ligated into the pMAL-c5x vector. The sequences of all constructed plasmids were confirmed by sequencing, and then transformed into *E. coli* BL21(DE3) for protein expression. Single colonies of transformed *E. coli* were picked and cultured in 5 mL of LB medium supplemented with antibiotic (50 μg/ml kanamycin for pET28a, 100 μg/ml ampicillin for pMAL-c5x) overnight in a

411 shaking incubator at 37 °C. The overnight culture was then expanded at a 1:100 ratio in 2x YT
412 medium with antibiotic and cultured at 37 °C. After the OD_{600} reached 0.5 to 0.7, the culture was
413 induced with 50 μM isopropyl-D-thiogalactopyranoside for 12-16 hrs at room temperature.
414 Bacteria pellets collected by centrifugation at 6,000 *x* g for 10 min, and frozen at -80 °C. Thawed
415 *E. coli* pellets were resuspended in 10 mL of buffer containing 20 mM Tris pH 7.5 and 500 mM
416 NaCl, and then lysed by sonication. Cell lysates were centrifuged at 12,000 x g for 30 min and
417 the supernatant was subsequently used for protein purification through a HisTrap column (His-
418 tagged full-length proteins, GE Healthcare) or Amylose resin (MBP-tagged fragments, New
419 England Biolabs) following the manufacturer's protocols.
420

Table 2. Summary of primers used for cloning of PspA and PhtD genes.

Primer	Sequences (5' → 3')
PspA1-F	CGC**CATATG**atggctaataagaaaaaaatgatttt
PspA247-F	CGC**CATATG**gagctaaacgctaaacaa
PspA436-F	CGC**CATATG**gatgaagaagaaactccagcg
PspA438-R	TAG**CGGCCG**TTAATGGTGATGGTGATGGTGttcttcatctccatcagggc
PspA512-R	TAG**CGGCCG**TTAATGGTGATGGTGATGGTGttttggagtggctggtttttc
PspA725-R	TAG**CGGCCG**TTAATGGTGATGGTGATGGTGaacccattcaccattggcat
PhtD1-F	CATG**CCATGG**CCatgaaaatcaataaaaaatatctagcagg
PhtD168-F	CATG**CCATGG**CCgcagataatgctgttgctg
PhtD341-F	CATG**CCATGG**CCtatcgttcaaaccattgggt
PhtD645-F	CATG**CCATGG**CCgaccattaccataacatcaaatttg
PhtD170-R	CCC**AAGCTT**TTAATGGTGATGGTGATGGTGattatctgctcttgagttatgattatg
PhtD343-R	CCC**AAGCTT**TTAATGGTGATGGTGATGGTGtgaacgataacgaaggggaat
PhtD647-R	CCC**AAGCTT**TTAATGGTGATGGTGATGGTGgtaatggtcataatgaggtatgatta aa

PhtD838-R	CCC**AAGCTT**TTAATGGTGATGGTGATGGTGctgtataggagccggttga
*Restriction enzyme sites are in bold, His-tags are underlined.	

421

422 Enzyme-linked immunosorbent assay for binding to pneumococcal proteins

423 For recombinant protein capture ELISA assays, 384-well plates were treated with 2 µg/ml of
424 antigen in PBS for 1 hr at 37 °C or overnight at 4 °C. Following this, plates were washed once
425 with distilled water before blocking for 1 hr with 2% nonfat milk/2% goat serum in 0.05% PBS-T
426 (blocking buffer). Plates were washed with water three times before applying serially diluted
427 primary mAbs in PBS for 1 hr. Following this, plates were washed with water three times before
428 applying 25 µL of secondary antibody (goat anti-human IgG Fc; Meridian Life Science) at a
429 dilution of 1:4,000 in blocking solution. After incubation for 1 hr, the plates were washed five
430 times with PBS-T, and 25 µL of a PNPP (p-nitrophenyl phosphate) solution (1 mg/ml PNPP in
431 1 M Tris base) was added to each well. The plates were incubated at room temperature for
432 1 hr before reading the optical density at 405 nm on a BioTek plate reader. Binding assay
433 data were analyzed in GraphPad Prism using a nonlinear regression curve fit and the
434 log(agonist)-versus-response function to calculate the binding EC_{50} values.

435

436 Generation of pneumococcal-specific hybridomas

437 For hybridoma generation, 10 million peripheral blood mononuclear cells purified from the blood
438 of human donors were mixed with 8 million previously frozen and gamma irradiated NIH 3T3
439 cells modified to express human CD40L, human interleukin-21 (IL-21), and human BAFF(71) in
440 80 mL StemCell medium A (StemCell Technologies) containing 6.3 µg/mL of CpG
441 (phosphorothioate-modified oligodeoxynucleotide ZOEZOEZZZZZOEEZOEZZZT, Invitrogen)
442 and 1 µg/mL of cyclosporine A (Millipore-Sigma). The mixture of cells was plated in four 96-well
443 plates at 200 µl per well in StemCell medium A. After 6 days, culture supernatants were
444 screened by ELISA for binding to recombinant pneumococcal protein, and cells from positive

445 wells were electrofused to generate hybridomas and biologically cloned as previously described
446 (71).
447
448 Human mAb expression and purification
449 For hybridoma-derived mAbs, hybridoma cell lines were expanded in StemCell medium A until
450 80% confluent in 75-cm^2 flasks. Cells from one 75-cm^2 cell culture flask were collected with a
451 cell scraper and expanded to 225-cm^2 cell culture flasks in serum-free medium (Hybridoma-
452 SFM; Thermo Fisher Scientific). Recombinant cultures from transfection were stopped after 5 to
453 7 days, and hybridoma cultures were stopped after 30 days. For recombinant PhtD3-IgG_{2a},
454 plasmids encoding cDNAs for the heavy and light chain sequences of PhtD3-IgG_{2a} were
455 synthesized (GenScript), and cloned into pCDNA3.1+. mAbs were obtained by transfection of
456 plasmids into Expi293F cells by transfection. For each milliliter of transfection, 1 µg of plasmid
457 DNA was mixed with 4 µg of 25,000-molecular-weight polyethylenimine (PEI; PolySciences Inc.)
458 in 66.67 µL Opti-MEM cell culture medium (Gibco). After 30 min, the DNA-PEI mixture was
459 added to the Expi293F cells, and cells were cultured for 5-6 days for protein expression. Culture
460 supernatants from both approaches were filtered using 0.45 µm filters to remove cell debris.
461 mAbs were purified directly from culture supernatants using HiTrap protein G columns (GE
462 Healthcare Life Sciences) according to the manufacturer's protocol.
463
464 Isotype determination for human mAbs
465 For determination of mAb isotypes, 96-well Immulon 4HBX plates (Thermo Fisher Scientific)
466 were coated with 2 µg/mL of each mAb in PBS (duplicate wells for each sample). The plates
467 were incubated at 4 °C overnight and then washed once with water. Plates were blocked with
468 blocking buffer and then incubated for 1 hr at room temperature. After incubation, the plates
469 were washed three times with water. Isotype-specific antibodies obtained from Southern Biotech
470 (goat anti-human kappa-alkaline phosphatase [AP] [catalog number 100244-340], goat anti-

human lambda-AP [catalog number 100244-376], mouse anti-human IgG1 [Fc]-AP [catalog number 100245714], mouse anti-human IgG2 [Fc]-AP [catalog number 100245-734], mouse anti-human IgG3 [hinge]-AP [catalog number 100245-824], and mouse anti-human IgG4 [Fc]-AP [catalog number 100245-812]) were diluted 1:1,000 in blocking buffer, and 50 µl of each solution was added to the respective wells. Plates were incubated for 1 h at room temperature and then washed five times with PBS-T. The PNPP substrate was prepared at 1 mg/mL in substrate buffer (1 M Tris base, 0.5 mM $MgCl_2$, pH 9.8), and 100 µl of this solution was added to each well. Plates were incubated for 1 hr at room temperature and read at 405 nm on a BioTek plate reader.

RT-PCR for hybridoma mAb variable gamma chain and variable light chain.

RNA was isolated from expanded hybridoma cells using the ENZA total RNA kit (Omega BioTek) according to the manufacturer's protocol. cDNA was obtained using the Superscript IV Reverse Transcriptase kit. Following this, PCR was conducted in two steps using established primers for the heavy chain, and kappa and lambda light chains (87). Samples were analyzed by agarose gel electrophoresis and purified PCR products (ENZA cycle pure kit; Omega Bio-Tek) were cloned into the pCR2.1 vector using the Original TA cloning kit (Thermo Fisher Scientific) according to the manufacturer's protocol. Plasmids were purified from positive DH5α colonies with ENZA plasmid DNA mini kit (Omega Bio-Tek) and submitted to Genewiz for sequencing. Sequences were analyzed using IMGT/V-Quest (88).

Experimental setup for biolayer interferometry

For all biosensors, an initial baseline in running buffer (PBS, 0.5% bovine serum albumin [BSA], 0.05% Tween 20, 0.04% thimerosal) was obtained. For epitope mapping, 100 µg/mL of His-tagged PhtD protein was immobilized on anti-penta-HIS biosensor tips (FortéBio) for 120 s. For binding competition, the baseline signal was measured again for 60 s before biosensor tips

were immersed into wells containing 100 µg/mL of primary antibody for 300 s. Following this, biosensors were immersed into wells containing 100 µg/mL of a second mAb for 300 s. Percent binding of the second mAb in the presence of the first mAb was determined by comparing the maximal signal of the second mAb after the first mAb was added to the maximum signal of the second mAb alone. mAbs were considered noncompeting if maximum binding of the second mAb was ≥66% of its uncompeted binding. A level of between 33% and 66% of its uncompeted binding was considered intermediate competition, and ≤33% was considered competition.

Bacterial strains and growth conditions

Pneumococcal strains were grown at 37 °C in 5% CO_2 in Todd-Hewitt broth (BD, Franklin Lakes NJ) supplemented with 0.5% yeast extract for 12 hrs. Ten percent glycerol was added to the media and 500 µL aliquots were made. Cultures were kept at -80 °C until used, cultures were washed twice with PBS before being used in experiments. Colonies were grown on BD Trypticase Soy Agar II with 5% Sheep Blood (BD, Franklin Lakes NJ). The numbers of CFUs per milliliter of these stocks were determined, after the aliquots had been frozen, by plating a single quick-thawed diluted aliquot on sheep's blood agar plates. The calculated number of CFUs was subsequently used to make dilutions for experiments from aliquots thawed at later times. In each experiment, the actual number of CFUs administered was determined by plating on blood agar at the time of the assay. Strains used in this study are listed in **Table 3**.

Table 3. Summary of pneumococcal strains used in this study.

Pneumococcal Strain	**Serotype**	**Source**
SPEC 1	1	BEI NR-13388
STREP2	2	BEI NR-31700
WU2	3	Gift from Dr. Moon Nahm, University of

		Alabama Birmingham
TIGR4	4	Gift from Dr. Larry McDaniel, University of Mississippi Medical Center
SPEC6C	6C	BEI NR-20805
SPEC6D	6D	BEI NR-20806
STREP8	8	BEI NR-31701
SPEC9N	9N	BEI NR-31702
OREP10A	10A	BEI NR-31703
TREP11A	11A	BEI NR-31705
TREP12F	12F	BEI NR-31704
TREP15B	15B	BEI NR-33666
OREP17F	17F	BEI NR-31706
TCH8431	19A	BEI HM-145
SPEC20B	20B	BEI NR-33664
TREP22F	22F	BEI NR-31707
STREP33F	33F	BEI NR-33665

Western blot

Pneumococcal strains were mixed with non-reducing loading buffer (Laemmli SDS sample buffer, non-reducing 6X) and loaded on a 4-12% Bis-Tris gel (Invitrogen). Samples were then transferred to PVDF membranes via iBlot system (Invitrogen) and then blocked with 5% blocking buffer (5% nonfat milk in PBS-T) for 1 hr at room temperature or at 4°C overnight. The membrane was washed three times in five-minute intervals on an orbital shaker with 0.05% PBS-T. Then, primary antibodies were added at dilutions of 1 µg/mL in PBS for one hour at room temperature. The membranes were then washed three time in five-minute intervals with

PBS-T on an orbital shaker, and soaked in the secondary antibody at a 1:8,000 dilution in blocking buffer for one hour. Next, the membranes were then washed five times in five-minute intervals on the orbital shaker with PBS-T, and substrate (Pierce ECL Western Blotting Substrate, Thermo Scientific) was added and an image was taken immediately with the ChemiDoc Imaging System (BioRad).

Enzyme-linked immunosorbent assay of fixed pneumococcus.

384-well plates were treated with 15 µL (~10^7 CFUs) of whole cell pneumococcus in PBS into each well. Cell density was checked by microscope to ensure a confluent layer of pneumococcus was coated. The bacteria were then fixed with 15 µl of 4% paraformaldehyde into each well and placed onto a plate shaker for 10 mins to mix. The 384-well plates were incubated at 4 °C for 24-48 hours to allow the bacteria to fix to the bottom of the plates. Following this, the plates were washed once with 75 µl of PBS-T into each well. The plates were then blocked with 2% blocking buffer for 1 hr at room temperature then washed three times with PBS-T. Next, 25 µl of serially diluted primary antibodies were applied to the wells for 1 hr at room temperature, then plates were washed with PBS-T three times. Following this, 25 µl of secondary antibody (goat anti-human IgG Fc; Meridian Life Science) at a 1:4,000 dilution in blocking buffer was applied to each well for 1 hr at room temperature. After the plates were washed with PBS-T five times, 25 µl of PNPP (p-nitrophenyl phosphate) solution (1 mg/ml PNPP in 1 M Tris bases) was added to each well for 1 hr at room temperature. After 1 hr the optical density was read at 405 nm on a BioTek plate reader. Binding assay data were analyzed in GraphPad Prism.

Binding of antibodies to bacteria by flow cytometry

The ability of mAbs to bind antigen exposed on the surface of *S. pneumoniae* was determined by flow cytometry. Bacteria were stained with 10 µM CFSE (Millipore Sigma) for

1 hr at 37 ºC. Bacteria were then washed with Hank's Balanced Salt Solution (HBSS) containing 1% bovine serum albumin (BSA) to remove excess stain. Following this, $1x10^6$ bacteria were incubated with 10 µg/ml of antibody for 30 min at 37 ºC. Bacteria were then washed twice with HBSS+1% BSA. Antibody binding was detected using an APC Anti-Human IgG Fc (Biolegend) at a 1:100 dilution incubated for 1 hr with the bacteria. Cells were washed with HBSS+1% BSA and fixed in 2% paraformaldehyde (PFA) in PBS prior to analysis on a NovoCyte Quanteon Flow Cytometer.

Determination of mAb efficacy

For intranasal challenge study with TIGR4, 5-7-week-old CBA/CaHN-Btkxid/J (CBA/N) mice (The Jackson Laboratory, Bar Harbor, ME) were used. Mice were intraperitoneally inoculated with antibody treatments 2 hrs prior to pneumococcal infection. For infection, mice were anesthetized by inhalation of 5% isoflurane and intranasally challenged with 40 µL of PBS containing 10^5 colony-forming units (CFUs) of TIGR4. Mice were weighed and assessed daily, and were considered moribund when >20% of body weight was lost or they were nonresponsive to manual stimulation or exhibited respiratory distress. Mice were euthanized by CO_2 asphyxiation followed by cervical dislocation. For the intravenous challenge with TIGR4, C57BL/6 mice 5-7 weeks old (Charles River) were used. Mice were intraperitoneally inoculated with antibody treatments two hrs prior to pneumococcal infection, and infected intravenously with 10^6 CFUs of TIGR4 via the tail vein. Mice were monitored and euthanized as described above. For intranasal challenge studies with WU2, C57BL/6 mice 5-7 weeks old (Charles River) were used. For intranasal infection, mice were anesthetized by inhalation of 5% isoflurane and intranasally challenged with 40 µL of PBS containing 10^6 colony-forming units (CFUs) of WU2. Mice were either treated 2 hrs before infection or 24 hours post infection by intraperitoneally inoculating with antibody. In prophylactic studies, mice were euthanized based on the humane

577 endpoints above. For treatment studies, mice were euthanized when >30% of pre-infection body
578 weight was lost or they were nonresponsive to manual stimulation or exhibited respiratory
579 distress. Actual doses delivered to mice in all studies were determined by titering the bacteria
580 after delivery.
581
582 Opsonophagocytic killing assay
583 An opsonophagocytic killing assay was performed as described previously (89, 90) as adapted
584 from an earlier protocol with modifications (91). TIGR4 stocks were incubated in triplicate wells
585 in a 96-well round-bottom plate for 1 hour at 37°C with the indicated antibodies (10 µg of
586 antibody per well in a final volume of 100 µL per well) in opsonization buffer B (OBB: sterile 1×
587 PBS with Ca^{2+}/Mg^{2+}, 0.1% gelatin, and 5% heat-inactivated FetalClone [HyClone]), with heat-
588 inactivated FetalClone-treated only TGR4 cells serving as a control. Cells of the human
589 promyelocytic leukemia cell line HL-60 (ATCC) were cultured in RPMI with 10% heat-inactivated
590 FetalClone and 1% l-glutamine. HL-60 cells were differentiated using 0.6% *N*,*N*-
591 dimethylformamide (DMF [Fisher]) for 3 days before performing the OPA assay, harvested, and
592 resuspended in OBB. Baby rabbit complement (Pel-Freez) was added to HL-60 cells at a 1:5
593 final volume. The HL-60–complement mixture was added to the bacteria at 5×10^5 cells/well.
594 The final reaction mixtures were incubated at 37°C for 1 hour with shaking. The reactions were
595 stopped by incubating the samples on ice for approximately 20 min. Then 10 µL of each
596 reaction mixture (triplicate) was diluted to a final volume of 50 µL and plated onto blood agar
597 plates. Plates were incubated overnight at 30°C and counted the next day. The percentage of
598 bacterial killing was calculated as each sample replicate normalized to the mean value obtained
599 for the control samples, subtracted from 100 (with No Ab control samples representing 0%
600 survival).
601
602 Flow-based opsonophagocytosis assay

603 Pneumococcal cells were stained with pHRodo Succinimidyl Ester (Invitrogen) following
604 manufacturer's protocol. Approximately, ~10^8 CFUs of bacteria were fixed with 1%
605 paraformaldehyde in PBS for 30 min at room temperature. Fixed bacteria were washed twice
606 with PBS and resuspended with 0.5 mL freshly prepared 100 mM $NaHCO_3$ (pH 8.5).
607 Immediately before use, the contents of a 0.1 mg vial of pHRodo iFL amine-reactive dye were
608 dissolved in 10 µL of DMSO to prepare a 10 mM stock solution. pHRodo was diluted in the
609 bacterial suspension at a final concentration of 0.1 mM, and bacteria were stained for 1 hr at
610 room temperature. Stained bacteria were washed twice with Hank's Balanced Salt Solution with
611 Ca^{2+} and Mg^{2+} (HBSS, Gibco), and resuspended with 0.5 mL HBSS and stored in the dark at 4
612 °C. The opsonophagocytosis assay was performed in 96 well U-bottom plates in a total volume
613 of 120 µL per well. First, 20 µL of pHRodo labeled bacteria (~10^7 CFUs/well) was mixed with 40
614 µL of sterile filtered mAbs (50 µg/well), and incubated on a shaker at 37 °C for 30 min. Bacteria
615 were mixed with HBSS as a negative control, and purified human serum IgG was used as a
616 positive control. Differentiated HL-60 cells were washed twice with HBSS and mixed with baby
617 rabbit complement (Pel-Freez Biologicals) at a final concentration of 10% in each well.
618 Following this, 60 µL (1×10^6 viable cells) of differentiated HL60 cells and complement were
619 added to the mixture of bacteria and antibodies, and incubated on a shaker at 37 °C for 60 min.
620 The plate was then centrifuged at 1300 rpm for 5 min at 4 °C to remove the supernatant and the
621 pellet was washed twice with 200 µL of HBSS. After the second wash, the pellet was
622 resuspended in a 50 µL mixture of PE-anti-human CD11b (Southern Biotech, 10 µL/million
623 cells), Alexa Fluor 647-anti-human CD35 (BD Biosciences, 5 µL/million cells), and DAPI
624 (Invitrogen, 50 ng/million cells) in PBS containing 1% BSA. After a 30 min incubation at 4 °C in
625 the dark, the plate was washed twice with 200 µL of PBS, and cells were resuspended in 100
626 µL of PBS. Cells were analyzed with a NovoCyte Quanteon Flow Cytometer. Single fluorophore
627 stained differentiated HL60 cells and pHRodo stained bacteria were used to calculate the

628 compensation matrix. A total of 10,000 ungated events were collected from each sample well,
629 and data were analyzed by FlowJo.
630

631 **Acknowledgements**

632 These studies were supported by startup funding from the University of Georgia Office of the
633 Vice President for Research, a Junior Faculty Seed Grant from the University of Georgia Office
634 of Research, and National Institutes of Health grants 1K01OD026569 (JJM) and R01AI123383
635 (FYA). Human subject studies were partially funded by the National Center for Advancing
636 Translational Sciences award number UL1TR002378. FR was supported by National Institutes
637 of Health NIGMS grant GM109435, Post-Baccalaureate Training in Infectious Diseases
638 Research. The funders had no role in study design, data collection and analysis, decision to
639 publish, or preparation of the manuscript. The content is solely the responsibility of the authors
640 and does not necessarily represent the official views of the National Institutes of Health. We
641 thank the University of Georgia Clinical and Translational Research Unit for assistance with
642 donor identification and blood draws, and the University of Georgia Center for Tropical and
643 Emerging Global Diseases and College of Veterinary Medicine flow cytometry cores for
644 assistance with cell sorting and analysis.

645

646 **Disclosure**

647 J.H, A.D.G., F.R., F.Y.A., and J.J.M. are inventors on a provisional patent application filed
648 describing the sequences of the monoclonal antibodies.

649

650 **Figure 1. Antibody responses and mAb binding properties to recombinant PhtD and**
651 **PspA proteins.** (A) SDS-PAGE (left) and western blot (right) of purified recombinantly
652 expressed PspA and PhtD. Both proteins were pure with the appearance of degradation
653 products. (B) ELISA binding responses from the supernatant of stimulated B cells to
654 recombinant PhtD and PspA proteins. (C) ELISA binding curves of anti-PhtD mAbs against
655 recombinant PhtD protein. PspA16 was utilized as a negative control. > indicates no binding
656 was observed at an OD_{405} over 1 Abs at the highest concentration. (D) Binding of PspA16 to
657 recombinant PspA. For (C) and (D), computed EC_{50} values in ng/mL are reported from a non-
658 linear regression curve fit (agonist). Data points indicate the average of four replicates from one
659 of at least two independent experiments. Error bars indicate 95% confidence intervals.

Table 1. Summary of genetic characteristics of pneumococcal-specific mAbs.

mAb	isotype	V_H gene (% mutation)	D_H	J_H	HCDR3 sequence	V_L (% mutation)	J_L	LCDR3 sequence
PhtD3	IgG_1, k	V1-69*18 (85%)	D3-16*01	J3*01	ARDGHIMRTTLSDAALDV	V3-20*01 (91%)	J4*01	QQYQNSPFT
PhtD6	IgG_1, k	V1-8*01 (93%)	D2-15*01	J5*02	ARGPYWVENWFDT	V1-39*01 (92%)	J1*01	QQSYSNQKT
PhtD7	IgG1, λ	V1-2*02 (91%)	D3-16*01	J4*02	ARVLRGSYDFRGNYPHDFDY	V4-69*01 (88%)	J3*02	QTWDTGLQGV
PhtD8	IgG_1, λ	V1-2*02 (93%)	D2-15*01	J4*02	ARGGTLDH	V4-69*01 (94%)	J3*02	HTWVTNIHLV
PspA16	IgG_1, k	V1-2*02 (93%)	D3-10*01	J1*01	ARAWAPGAEYLHH	V3-20*01 (94%)	J3*01	QQHDHSPFT

Analysis was performed using IMGT/V-Quest.

660

Figure 2. Epitope mapping of anti-PhtD mAbs. (A) SDS-PAGE of the purified maltose binding protein (MBP) PhtD fragment fusion proteins. Each fusion protein was pure after purification with the exception of free MBP. (B) ELISA binding curves of the PhtD mAbs to each MBP-PhtD fragment. A summary of the binding curves is displayed below the binding curves, where cells colored in blue indicate binding, and those colored in white indicate no binding. Data points indicate the average of four replicates from one of at least two independent experiments. Error bars indicate 95% confidence intervals. (C) An example of an epitope mapping experiment for the anti-PhtD mAbs. The top graph displays the signal from biolayer interferometry of the first mAb loaded onto immobilized PhtD protein. The signal for each mAb is colored according to the legend. The bottom graph displays the signal from loading of the second mAb in the presence of the first mAb, mAb PhtD3 in this example. A decrease in signal compared to the top graph is observed for mAbs PhtD3 and PhtD8, as mAb PhtD3 competes with itself, and mAbs PhtD3 and PhtD6 have partially overlapping epitopes. (D) Epitope mapping of the PhtD-specific mAbs. Data indicate the percent binding of the competing antibody in the presence of the primary antibody, compared with the competing antibody alone. Cells filled in black indicate full competition, in which ≤33% of the uncompeted signal was observed; cells in gray indicate intermediate competition, in which the signal was between 33% and 66%; and cells in white indicate noncompetition, where the signal was ≥66%.

680 **Figure 3. Epitope mapping of PspA16.** (A) SDS-PAGE of recombinant MBP PspA fragment
681 fusion proteins. Fragments 1-2 and 4-5 purified well, with only visible MBP protein as a
682 contaminant. PspA fragment 3 has multiple co-purified bands and/or degradation products. (B)
683 ELISA binding curves for PspA16 to each fragment. PspA16 bound to fragment 1 and fragment
684 4, but not others, suggesting the epitope lies within amino acids 1-247. Data points indicate the
685 average of four replicates from one of at least two independent experiments. Error bars indicate
686 95% confidence intervals.
687

688 **Figure 4. Serotype breadth of the isolated mAbs.** (A) Western blot of TIGR4 and TCH8431
689 strains with PspA16 and PhtD3 as the primary antibodies. In the western blot for PspA16, PspA
690 fragment 1-438 fused to the MBP was used as the positive control, and MBP was used as the
691 negative control. In the PhtD3 western blot, recombinant PhtD was used as the positive control,
692 and *E. coli* lysates were used as the negative control. (B) Area under the curve (AUC) values
693 calculated from ELISA binding curves of serially diluted mAbs against plates coated with fixed
694 bacteria. The ELISA binding curves were the the average of four data points from one of at least
695 two independent experiments. The baseline for the AUC calculation was set as the average of
696 the signal for the highest concentration (20 μg/mL) of the negative control mAb MPV314. Error
697 bars are the standard error from the AUC calculation. (C) Example gating strategy for antibody
698 binding to bacteria. Bacteria were labeled with CFSE, and antibodies were labeled with APC.
699 (D) Heat map and percentages for antibody binding to each pneumococcal serotype. Data are
700 averages from 3-4 experiments, and are the percent of bacteria that are APC-positive. MPV314
701 and MPV414 are human antibodies specific to the human metapneumovirus fusion protein, and
702 these were used as negative controls.
703

Figure 5. Protective efficacy of anti-PhtD mAbs. (A) ELISA binding curve of mAb PhtD3, the isotype-switched mAb PhtD-IgG_{2a}, and an IgG_{2a} isotype control. Data points indicate the average of four replicates from one of at least two independent experiments. Error bars indicate 95% confidence intervals. (B) Prophylactic efficacy of mAb PhtD3 in an intranasal infection model of pneumococcal serotype 3 (strain WU2) in C57BL/6 mice. **, P=0.0012, ns=not significant via log-rank (Mantel-Cox) test. n=10 mice/group. (C) Prophylactic efficacy of mAb PhtD8 in an intranasal infection model of pneumococcal serotype 3 (strain WU2) in C57BL/6 mice. ***, P=0.0009, ns=not significant via log-rank (Mantel-Cox) test. n=10 mice/group. (C) Prophylactic efficacy of mAb PhtD3 in an intranasal infection model of pneumococcal serotype 4 (strain TIGR4) in CBA/N mice. **, P=0.0045 via log-rank (Mantel-Cox) test. n=15 mice/group. (D) Prophylactic efficacy of mAb PhtD3 in an intravenous infection model of pneumococcal serotype 4 (strain TIGR4) in C57BL/6 mice. **P=0.0101 via log-rank (Mantel-Cox) test. n=13-15 mice/group. (E) Treatment efficacy of mAb PhtD3 in an intranasal infection model of pneumococcal serotype 3 (strain WU2) in C57BL/6 mice. ***P=0.0002, ns=not significant via log-rank (Mantel-Cox) test. n=20 mice/group.

721 **Figure 6. Opsonophagocytic activity of PhtD-specific human mAbs.** (A) mAbs and serum
722 were tested in a standard OPA assay using differentiated HL-60 cells. Bacteria were opsonized
723 with antibodies, and subsequently HL-60 cells were added before plating onto blood agar
724 plates. Plates were incubated overnight and CFUs counted. Data are averages of three
725 replicates from one experiment. Error bars represent the range. % Bacterial Killing was
726 calculated as the counted CFU value of each triplicate normalized against the average of the No
727 Ab control. One-way ANOVA analysis with Dunnett's multiple comparisons test was used to
728 determine significance. ns=not significant, ****P<0.0001. (B) mAbs and serum were tested in a
729 flow-based opsonophagocytosis assay. pHRodo-labeled bacteria were opsonized with
730 antibodies, and incubated with HL-60 cells before being subjected to analysis by flow cytometry.
731 Data indicate the percent of CD38+CD11b+ HL-60 cells that are pHRodo+. Each bar graph is
732 the average of three experimental replicates and error bars are the standard deviation. ns=not
733 significant, ***P=0.0001-0.0006, ****P<0.0001 via one-way ANOVA analysis with Dunnett's
734 multiple comparisons test. MPV414 is a human mAb specific to the human metapneumovirus
735 fusion protein.
736

References

1. Levine OS, O'Brien KL, Knoll M, Adegbola RA, Black S, Cherian T, Dagan R, Goldblatt D, Grange A, Greenwood B, Hennessy T, Klugman KP, Madhi SA, Mulholland K, Nohynek H, Santosham M, Saha SK, Scott JA, Sow S, Whitney CG, Cutts F. 2006. Pneumococcal vaccination in developing countries. Lancet 367:1880–1882.
2. WHO. 2003. Pneumococcal vaccines. Wkly Epidemiol Rec 78:110–119.
3. Practices AC on I. 2000. Preventing pneumococcal disease among infants and young children. MMWR Recomm Rep 49:1–35.
4. van der Poll T, Opal SM. 2009. Pathogenesis, treatment, and prevention of pneumococcal pneumonia. Lancet 374:1543–1556.
5. Bridy-Pappas AE, Margolis MB, Center KJ, Isaacman DJ. 2005. Streptococcus pneumoniae: description of the pathogen, disease epidemiology, treatment, and prevention. Pharmacotherapy 25:1193–212.
6. Williams BG, Gouws E, Boschi-pinto C, Bryce J, Dye C. 2002. Estimates of world-wide distribution of child deaths from acute respiratory infections died from ARI in 2000 , 70 % of them in Africa and. Lancet Infect Dis 2:25–32.
7. Sulikowska A, Grzesiowski P, Sadowy E, Fiett J, Hryniewicz W. 2004. Characteristics of Streptococcus pneumoniae, Haemophilus influenzae, and Moraxella catarrhalis isolated from the nasopharynges of asymptomatic children and molecular analysis of S. pneumoniae and H. influenzae strain replacement in the nasopharynx. J Clin Microbiol 42:3942–3949.
8. Simell B, Auranen K, Käyhty H, Goldblatt D, Dagan R, O'Brien KL. 2012. The fundamental link between pneumococcal carriage and disease. Expert Rev Vaccines 11:841–855.
9. Cardozo DM, Nascimento-Carvalho CM, Andrade AL, Silvany-Neto AM, Daltro CH,

763 Brandao MA, Brandao AP, Brandileone MC. 2008. Prevalence and risk factors for
764 nasopharyngeal carriage of Streptococcus pneumoniae among adolescents. J Med
765 Microbiol 57:185–189.
766 10. Shrestha S, Foxman B, Weinberger DM, Steiner C, Viboud C, Rohani P. 2013. Identifying
767 the interaction between influenza and pneumococcal pneumonia using incidence data.
768 Sci Transl Med 5:191ra84-191ra84.
769 11. Zhu X, Ge Y, Wu T, Zhao K, Chen Y, Wu B, Zhu F, Zhu B, Cui L. 2020. Co-infection with
770 respiratory pathogens among COVID-2019 cases. Virus Res 285:198005.
771 12. Weinberger DM, Dagan R, Givon-Lavi N, Regev-Yochay G, Malley R, Lipsitch M. 2008.
772 Epidemiologic evidence for serotype-specific acquired immunity to pneumococcal
773 carriage. J Infect Dis 197:1511–1518.
774 13. Goldblatt D, Hussain M, Andrews N, Ashton L, Virta C, Melegaro A, Pebody R, George R,
775 Soininen A, Edmunds J, Gay N, Kayhty H, Miller E. 2005. Antibody responses to
776 nasopharyngeal carriage of Streptococcus pneumoniae in adults: a longitudinal
777 household study. J Infect Dis 192:387–93.
778 14. McCool TL, Cate TR, Moy G, Weiser JN. 2002. The immune response to pneumococcal
779 proteins during experimental human carriage. J Exp Med 195:359–365.
780 15. Prevaes SM, van Warmel WJ, de Vogel CP, Veenhoven RH, van Gils EJ, van Belkum A,
781 Sanders EA, Bogaert D. 2012. Nasopharyngeal colonization elicits antibody responses to
782 staphylococcal and pneumococcal proteins that are not associated with a reduced risk of
783 subsequent carriage. Infect Immun 80:2221-2186–2193.
784 16. Turner P, Turner C, Green N, Ashton L, Lwe E, Jankhot A, Day NP, White NJ, Nosten F,
785 Goldblatt D. 2013. Serum antibody responses to pneumococcal colonization in the first 2
786 years of life: Results from an SE Asian longitudinal cohort study. Clin Microbiol Infect
787 19:E551–E558.
788 17. Zhang Q, Bernatoniene J, Bagrade L, Pollard AJ, Mitchell TJ, Paton JC, Finn A. 2006.

Serum and mucosal antibody responses to pneumococcal protein antigens in children: Relationships with carriage status. Eur J Immunol 36:46–57.

18. Mureithi MW, Finn A, Ota MO, Zhang Q, Davenport V, Mitchell TJ, Williams NA, Adegbola RA, Heyderman RS. 2009. T cell memory response to pneumococcal protein antigens in an area of high pneumococcal carriage and disease. J Infect Dis 200:783–793.

19. Wright AKA, Bangert M, Gritzfeld JF, Ferreira DM, Jambo KC, Wright AD, Collins AM, Gordon SB. 2013. Experimental human pneumococcal carriage augments IL-17A-dependent T-cell defence of the lung. PLoS Path e1003274.

20. Simell B, Lahdenkari M, Reunanen A, Käyhty H, Väkeväinen M. 2008. Effects of ageing and gender on naturally acquired antibodies to pneumococcal capsular polysaccharides and virulence-associated proteins. Clin Vacc Immunol 15:1391–1397.

21. Ganaie F, Saad JS, McGee L, van Tonder AJ, Bentley SD, Lo SW, Gladstone RA, Turner P, Keenan JD, Breiman RF, Nahm MH. 2020. A New Pneumococcal Capsule Type, 10D, is the 100th Serotype and Has a Large cps Fragment from an Oral Streptococcus. MBio 11:e00937-20.

22. Geno KA, Gilbert GL, Song JY, Skovsted IC, Klugman KP, Jones C, Konradsen HB, Nahm MH. 2015. Pneumococcal capsules and their types: Past, present, and future. Clin Microbiol Rev 28:871–899.

23. Chen Z, Cox KS, Tang A, Roman J, Fink M, Kaufhold RM, Guan L, Xie A, Boddicker MA, McGuinness D, Xiao X, Li H, Skinner JM, Verch T, Retzlaff M, Vora KA. 2018. Human monoclonal antibodies isolated from a primary pneumococcal conjugate vaccinee demonstrates the expansion of an antigen-driven hypermutated memory B cell response. BMC Infect Dis 18:613.

24. Wantuch PL, Avci FY. 2018. Current status and future directions of invasive pneumococcal diseases and prophylactic approaches to control them. Hum Vaccines

Immunother 14:2303–2309.

25. Linley E, Bell A, Gritzfeld JF, Borrow R. 2019. Should pneumococcal serotype 3 be included in serotype-specific immunoassays? Vaccines 7:doi: 10.3390/vaccines7010004.

26. Lo SW, Gladstone RA, van Tonder AJ, Lees JA, du Plessis M, Benisty R, Givon-Lavi N, Hawkins PA, Cornick JE, Kwambana-Adams B, Law PY, Ho PL, Antonio M, Everett DB, Dagan R, von Gottberg A, Klugman KP, McGee L, Breiman RF, Bentley SD, Brooks AW, Corso A, Davydov A, Maguire A, Pollard A, Kiran A, Skoczynska A, Moiane B, Beall B, Sigauque B, Aanensen D, Lehmann D, Faccone D, Foster-Nyarko E, Bojang E, Egorova E, Voropaeva E, Sampane-Donkor E, Sadowy E, Bigogo G, Mucavele H, Belabbès H, Diawara I, Moïsi J, Verani J, Keenan J, Nair Thulasee Bhai JN, Ndlangisa KM, Zerouali K, Ravikumar KL, Titov L, De Gouveia L, Alaerts M, Ip M, de Cunto Brandileone MC, Hasanuzzaman M, Paragi M, Nurse-Lucas M, Ali M, Elmdaghri N, Croucher N, Wolter N, Porat N, Köseoglu Eser Ö, Akpaka PE, Turner P, Gagetti P, Tientcheu PE, Carter PE, Mostowy R, Kandasamy R, Ford R, Henderson R, Malaker R, Shakoor S, Grassi Almeida SC, Saha SK, Doiphode S, Madhi SA, Devi Sekaran S, Srifuengfung S, Obaro S, Clarke SC, Nzenze SA, Kastrin T, Ochoa TJ, Balaji V, Hryniewicz W, Urban Y. 2019. Pneumococcal lineages associated with serotype replacement and antibiotic resistance in childhood invasive pneumococcal disease in the post-PCV13 era: an international whole-genome sequencing study. Lancet Infect Dis 19:759–769.

27. Daniels CC, Rogers PD, Shelton CM. 2016. A review of pneumococcal vaccines: Current polysaccharide vaccine recommendations and future protein antigens. J Pediatr Pharmacol Ther 21:27–35.

28. Lagousi T, Basdeki P, Routsias J, Spoulou V. 2019. Novel Protein-Based Pneumococcal Vaccines: Assessing the Use of Distinct Protein Fragments Instead of Full-Length Proteins as Vaccine Antigens. Vaccines 7:9.

29. Adamou JE, Heinrichs JH, Erwin AL, Walsh W, Gayle T, Dormitzer M, Dagan R, Brewah

YA, Barren P, Lathigra R, Langermann S, Koenig S, Johnson S. 2001. Identification and characterization of a novel family of pneumococcal proteins that are protective against sepsis. Infect Immun 69:949–958.

30. Rioux S, Neyt C, Di Paolo E, Turpin L, Charland N, Labbé S, Mortier MC, Mitchell TJ, Feron C, Martin D, Poolman JT. 2011. Transcriptional regulation, occurrence and putative role of the Pht family of Streptococcus pneumoniae. Microbiology 157:335–348.

31. Yun KW, Lee H, Choi EH, Lee HJ. 2015. Diversity of pneumolysin and pneumococcal histidine triad protein D of Streptococcus pneumoniae isolated from invasive diseases in Korean children. PLoS One 10:e0134055.

32. Kawaguchiya M, Urushibara N, Aung MS, Shinagawa M, Takahashi S, Kobayashi N. 2019. Prevalence of Various Vaccine Candidate Proteins in Clinical Isolates of Streptococcus pneumoniae: Characterization of the Novel Pht Fusion Proteins PhtA/B and PhtA/D. Pathog (Basel, Switzerland) 8:162.

33. Blumental S, Granger-Farbos A, Moïsi JC, Soullié B, Leroy P, Njanpop-Lafourcade B-M, Yaro S, Nacro B, Hallin M, Koeck J-L. 2015. Virulence Factors of Streptococcus pneumoniae. Comparison between African and French Invasive Isolates and Implication for Future Vaccines. PLoS One 10:e0133885.

34. Rioux S, Neyt C, Di Paolo E, Turpin L, Charland N, Labbé S, Mortier M-C, Mitchell TJ, Feron C, Martin D, Poolman JT. 2011. Transcriptional regulation, occurrence and putative role of the Pht family of Streptococcus pneumoniae. Microbiology 157:336–348.

35. Plumptre CD, Ogunniyi AD, Paton JC. 2013. Surface association of Pht proteins of Streptococcus pneumoniae. Infect Immun2013/07/22. 81:3644–3651.

36. Kallio A, Sepponen K, Hermand P, Denoël P, Godfroid F, Melin M. 2014. Role of Pht proteins in attachment of Streptococcus pneumoniae to respiratory epithelial cells. Infect Immun2014/02/03. 82:1683–1691.

37. Eijkelkamp BA, Pederick VG, Plumptre CD, Harvey RM, Hughes CE, Paton JC, McDevitt

867 CA. 2016. The First Histidine Triad Motif of PhtD Is Critical for Zinc Homeostasis in
868 Streptococcus pneumoniae. Infect Immun 84:407 LP – 415.
869 38. Luo Z, Pederick VG, Paton JC, McDevitt CA, Kobe B. 2018. Structural characterisation of
870 the HT3 motif of the polyhistidine triad protein D from Streptococcus pneumoniae. FEBS
871 Lett 592:2341–2350.
872 39. Bersch B, Bougault C, Roux L, Favier A, Vernet T, Durmort C. 2013. New Insights into
873 Histidine Triad Proteins: Solution Structure of a Streptococcus pneumoniae PhtD Domain
874 and Zinc Transfer to AdcAII. PLoS One 8:e81168.
875 40. Godfroid F, Hermand P, Verlant V, Denoël P, Poolman JT. 2011. Preclinical Evaluation of
876 the Pht Proteins as Potential Cross-Protective Pneumococcal Vaccine Antigens. Infect
877 Immun 79:238 LP – 245.
878 41. Wizemann TM, Heinrichs JH, Adamou JE, Erwin AL, Kunsch C, Choi GH, Barash SC,
879 Rosen CA, Masure HR, Tuomanen E, Gayle A, Brewah YA, Walsh W, Barren P, Lathigra
880 R, Hanson M, Langermann S, Johnson S, Koenig S. 2001. Use of a whole genome
881 approach to identify vaccine molecules affording protection against Streptococcus
882 pneumoniae infection. Infect Immun 69:1593–1598.
883 42. Denoël P, Philipp MT, Doyle L, Martin D, Carletti G, Poolman JT. 2011. A protein-based
884 pneumococcal vaccine protects rhesus macaques from pneumonia after experimental
885 infection with Streptococcus pneumoniae. Vaccine 29:5495–5501.
886 43. Plumptre CD, Ogunniyi AD, Paton JC. 2013. Vaccination against Streptococcus
887 pneumoniae Using Truncated Derivatives of Polyhistidine Triad Protein D. PLoS One
888 8:e78916.
889 44. André GO, Assoni L, Rodriguez D, Leite LCC, dos Santos TEP, Ferraz LFC, Converso
890 TR, Darrieux M. 2020. Immunization with PhtD truncated fragments reduces
891 nasopharyngeal colonization by Streptococcus pneumoniae. Vaccine 38:4146–4153.
892 45. Hammitt LL, Campbell JC, Borys D, Weatherholtz RC, Reid R, Goklish N, Moulton LH,

Traskine M, Song Y, Swinnen K, Santosham M, Brien KLO. 2019. Efficacy, safety and immunogenicity of a pneumococcal protein-based vaccine co-administered with 13-valent pneumococcal conjugate vaccine against acute otitis media in young children : A phase IIb randomized study. Vaccine https://do.

46. Visan L, Rouleau N, Proust E, Peyrot L, Donadieu A, Ochs M. 2018. Antibodies to PcpA and PhtD protect mice against Streptococcus pneumoniae by a macrophage- and complement-dependent mechanism. Hum Vaccin Immunother 14:489–494.

47. Kaur R, Surendran N, Ochs M, Pichichero ME. 2014. Human antibodies to PhtD, PcpA, and ply reduce adherence to human lung epithelial cells and murine nasopharyngeal colonization by Streptococcus pneumoniae. Infect Immun 82:5069–5075.

48. Brookes RH, Ming M, Williams K, Hopfer R, Gurunathan S, Gallichan S, Tang M, Ochs MM. 2015. Passive protection of mice against Streptococcus pneumoniae challenge by naturally occurring and vaccine-induced human anti-PhtD antibodies. Hum Vaccin Immunother 11:1836–1839.

49. Rosenow C, Ryan P, Weiser JN, Johnson S, Fontan P, Ortqvist A, Masure HR. 1997. Contribution of novel choline-binding proteins to adherence, colonization and immunogenicity of Streptococcus pneumoniae. Mol Microbiol 25:819–829.

50. Hollingshead SK, Baril L, Ferro S, King J, Coan P, Briles DE, Group TPPES. 2006. Pneumococcal surface protein A (PspA) family distribution among clinical isolates from adults over 50 years of age collected in seven countries. J Med Microbiol 55:215–221.

51. Briles DE, Yother J, McDaniel LS. 1988. Role of pneumococcal surface protein A in the virulence of Streptococcus pneumoniae. Rev Infect Dis 10 Suppl 2:S372-4.

52. Bosarge JR, Watt JM, McDaniel DO, Swiatlo E, McDaniel LS. 2001. Genetic immunization with the region encoding the alpha-helical domain of PspA elicits protective immunity against Streptococcus pneumoniae. Infect Immun 69:5456–5463.

53. McDaniel LS, Sheffield JS, Delucchi P, Briles DE. 1991. PspA, a surface protein of

Streptococcus pneumoniae, is capable of eliciting protection against pneumococci of more than one capsular type. Infect Immun 59:222–228.

54. McDaniel LS, McDaniel DO, Hollingshead SK, Briles DE. 1998. Comparison of the PspA sequence from Streptococcus pneumoniae EF5668 to the previously identified PspA sequence from strain Rx1 and ability of PspA from EF5668 to elicit protection against pneumococci of different capsular types. Infect Immun 66:4748–4754.

55. Kong IG, Sato A, Yuki Y, Nochi T, Takahashi H, Sawada S, Mejima M, Kurokawa S, Okada K, Sato S, Briles DE, Kunisawa J, Inoue Y, Yamamoto M, Akiyoshi K, Kiyono H. 2013. Nanogel-Based PspA Intranasal Vaccine Prevents Invasive Disease and Nasal Colonization by Streptococcus pneumoniae Infect Immun 81:1625 LP – 1634.

56. Piao Z, Akeda Y, Takeuchi D, Ishii KJ, Ubukata K, Briles DE, Tomono K, Oishi K. 2014. Protective properties of a fusion pneumococcal surface protein A (PspA) vaccine against pneumococcal challenge by five different PspA clades in mice. Vaccine 32:5607–5613.

57. Fukuyama Y, Yuki Y, Katakai Y, Harada N, Takahashi H, Takeda S, Mejima M, Joo S, Kurokawa S, Sawada S, Shibata H, Park EJ, Fujihashi K, Briles DE, Yasutomi Y, Tsukada H, Akiyoshi K, Kiyono H. 2015. Nanogel-based pneumococcal surface protein A nasal vaccine induces microRNA-associated Th17 cell responses with neutralizing antibodies against Streptococcus pneumoniae in macaques. Mucosal Immunol 8:1144–1153.

58. Arulanandam BP, Lynch JM, Briles DE, Hollingshead S, Metzger DW. 2001. Intranasal vaccination with pneumococcal surface protein A and interleukin-12 augments antibody-mediated opsonization and protective immunity against Streptococcus pneumoniae infection. Infect Immun 69:6718–6724.

59. Hollingshead SK, Becker R, Briles DE. 2000. Diversity of PspA: mosaic genes and

945 evidence for past recombination in Streptococcus pneumoniae. Infect Immun 68:5889–
946 5900.
947 60. Khan N, Jan AT. 2017. Towards Identifying Protective B-Cell Epitopes: The PspA Story .
948 Front Microbiol .
949 61. Ren B, Szalai AJ, Hollingshead SK, Briles DE. 2004. Effects of PspA and antibodies to
950 PspA on activation and deposition of complement on the pneumococcal surface. Infect
951 Immun 72:114–122.
952 62. Mukerji R, Mirza S, Roche AM, Widener RW, Croney CM, Rhee D-K, Weiser JN, Szalai
953 AJ, Briles DE. 2012. Pneumococcal surface protein A inhibits complement deposition on
954 the pneumococcal surface by competing with the binding of C-reactive protein to cell-
955 surface phosphocholine. J Immunol2012/10/26. 189:5327–5335.
956 63. Tu A-HT, Fulgham RL, McCrory MA, Briles DE, Szalai AJ. 1999. Pneumococcal Surface
957 Protein A Inhibits Complement Activation by Streptococcus pneumoniae. Infect Immun
958 67:4720 LP – 4724.
959 64. Håkansson A, Roche H, Mirza S, McDaniel LS, Brooks-Walter A, Briles DE. 2001.
960 Characterization of binding of human lactoferrin to pneumococcal surface protein A.
961 Infect Immun 69:3372–3381.
962 65. Senkovich O, Cook WJ, Mirza S, Hollingshead SK, Protasevich II, Briles DE,
963 Chattopadhyay D. 2007. Structure of a Complex of Human Lactoferrin N-lobe with
964 Pneumococcal Surface Protein A Provides Insight into Microbial Defense Mechanism. J
965 Mol Biol 370:701–713.
966 66. Nabors GS, Braun PA, Herrmann DJ, Heise ML, Pyle DJ, Gravenstein S, Schilling M,
967 Ferguson LM, Hollingshead SK, Briles DE, Becker RS. 2000. Immunization of healthy
968 adults with a single recombinant pneumococcal surface protein A (PspA) variant
969 stimulates broadly cross-reactive antibodies to heterologous PspA molecules. Vaccine
970 18:1743–1754.

971 67. Briles DE, Hollingshead SK, King J, Swift A, Braun PA, Park MK, Ferguson LM, Nahm
972 MH, Nabors GS. 2000. Immunization of Humans with Recombinant Pneumococcal
973 Surface Protein A (rPspA) Elicits Antibodies That Passively Protect Mice from Fatal
974 Infection with Streptococcus pneumoniae Bearing Heterologous PspA. J Infect Dis
975 182:1694–1701.
976 68. Wilcox MH, Gerding DN, Poxton IR, Kelly C, Nathan R, Birch T, Cornely OA, Rahav G,
977 Bouza E, Lee C, Jenkin G, Jensen W, Kim YS, Yoshida J, Gabryelski L, Pedley A, Eves
978 K, Tipping R, Guris D, Kartsonis N, Dorr MB. 2017. Bezlotoxumab for prevention of
979 recurrent Clostridium difficile infection. N Engl J Med 376:305–317.
980 69. Wilson R, Cohen JM, Reglinski M, Jose RJ, Chan WY, Marshall H, de Vogel C, Gordon
981 S, Goldblatt D, Petersen FC, Baxendale H, Brown JS. 2017. Naturally acquired human
982 immunity to pneumococcus Is dependent on antibody to protein antigens. PLoS Pathog
983 13:1–26.
984 70. Simell B, Ahokas P, Lahdenkari M, Poolman J, Henckaerts I, Kilpi TM, Käyhty H. 2009.
985 Pneumococcal carriage and acute otitis media induce serum antibodies to pneumococcal
986 surface proteins CbpA and PhtD in children. Vaccine 27:4615–4621.
987 71. Bar-Peled Y, Diaz D, Pena-Briseno A, Murray J, Huang J, Tripp RA, Mousa JJ. 2019. A
988 potent neutralizing site III-specific human antibody neutralizes human metapneumovirus
989 in vivo. J Virol 93:e00342-19.
990 72. Wantuch PL, Avci FY. 2019. Invasive pneumococcal disease in relation to vaccine type
991 serotypes. Hum Vaccin Immunother.
992 73. Sandgren A, Albiger B, Orihuela CJ, Tuomanen E, Normark S, Henriques-Normark B.
993 2005. Virulence in Mice of Pneumococcal Clonal Types with Known Invasive Disease
994 Potential in Humans. J Infect Dis 192:791–800.
995 74. Romero-Steiner S, Frasch CE, Carlone G, Fleck RA, Goldblatt D, Nahm MH. 2006. Use
996 of opsonophagocytosis for serological evaluation of pneumococcal vaccines. Clin

997 Vaccine Immunol 13:165–169.
998 75. Paschall A V, Middleton DR, Avci FY. 2019. Opsonophagocytic Killing Assay to Assess
999 Immunological Responses Against Bacterial Pathogens. JoVE e59400.
1000 76. Pilishvili T, Bennett NM. 2015. Pneumococcal disease prevention among adults:
1001 Strategies for the use of pneumococcal vaccines. Vaccine 33:D60–D65.
1002 77. Fabbrini M, Sammicheli C, Margarit I, Maione D, Grandi G, Giuliani MM, Mori E, Nuti S.
1003 2012. A new flow-cytometry-based opsonophagocytosis assay for the rapid measurement
1004 of functional antibody levels against Group B Streptococcus. J Immunol Methods
1005 378:11–19.
1006 78. Huang J, Diaz D, Mousa JJ. 2020. Antibody recognition of the Pneumovirus fusion
1007 protein trimer interface. PLOS Pathog 16:e1008942.
1008 79. Lagousi T, Routsias J, Piperi C, Tsakris A, Chrousos G, Theodoridou M, Spoulou V.
1009 2015. Discovery of Immunodominant B Cell Epitopes within Surface Pneumococcal
1010 Virulence Proteins in Pediatric Patients with Invasive Pneumococcal Disease. J Biol
1011 Chem2015/09/22. 290:27500–27510.
1012 80. McDaniel LS, Ralph BA, McDaniel DO, Briles DE. 1994. Localization of protection-
1013 eliciting epitopes on PspA of Streptococcus pneumoniae between amino acid residues
1014 192 and 260. Microb Pathog 17:323–337.
1015 81. Kolberg J, Aase A, Rødal G, Littlejohn JE, Jedrzejas MJ. 2003. Epitope mapping of
1016 pneumococcal surface protein A of strain Rx1 using monoclonal antibodies and molecular
1017 structure modelling. FEMS Immunol Med Microbiol 39:265–273.
1018 82. Hollingshead SK, Becker R, Briles DE. 2000. Diversity of PspA: Mosaic genes and
1019 evidence for past recombination in Streptococcus pneumoniae. Infect Immun 68:5889–
1020 5900.
1021 83. Keller LE, Robinson DA, McDaniel LS. 2016. Nonencapsulated Streptococcus
1022 pneumoniae: Emergence and Pathogenesis. MBio 7:e01792–e01792.

1023 84. Doyle CR, Pirofski L. 2016. Reduction of Streptococcus pneumoniae Colonization and
1024 Dissemination by a Nonopsonic Capsular Polysaccharide Antibody. MBio 7:e02260-15.
1025 85. Tian H, Weber S, Thorkildson P, Kozel TR, Pirofski LA. 2009. Efficacy of opsonic and
1026 nonopsonic serotype 3 pneumococcal capsular polysaccharide-specific monoclonal
1027 antibodies against intranasal challenge with streptococcus pneumoniae in mice. Infect
1028 Immun 77:1502–1513.
1029 86. Khan MN, Pichichero ME. 2012. Vaccine candidates PhtD and PhtE of Streptococcus
1030 pneumoniae are adhesins that elicit functional antibodies in humans. Vaccine2012/02/17.
1031 30:2900–2907.
1032 87. Guthmiller JJ, Dugan HL, Neu KE, Lan LY-L, Wilson PC. 2019. An Efficient Method to
1033 Generate Monoclonal Antibodies from Human B Cells BT - Human Monoclonal
1034 Antibodies: Methods and Protocols, p. 109–145. *In* Steinitz, M (ed.), . Springer New York,
1035 New York, NY.
1036 88. Brochet X, Lefranc MP, Giudicelli V. 2008. IMGT/V-QUEST: the highly customized and
1037 integrated system for IG and TR standardized V-J and V-D-J sequence analysis. Nucleic
1038 Acids Res 36:503–508.
1039 89. Middleton DR, Paschall A V, Duke JA, Avci FY. 2018. Enzymatic Hydrolysis of
1040 Pneumococcal Capsular Polysaccharide Renders the Bacterium Vulnerable to Host
1041 Defense. Infect Immun 86.
1042 90. Paschall AV, Middleton DR, Avci FY. 2019. Opsonophagocytic killing assay to assess
1043 immunological responses against bacterial pathogens. J Vis Exp 146:doi: 10.3791/59400.
1044 91. Burton RL, Nahm MH. 2012. Development of a fourfold multiplexed opsonophagocytosis
1045 assay for pneumococcal antibodies against additional serotypes and discovery of
1046 serological subtypes in Streptococcus pneumoniae serotype 20. Clin Vaccine
1047 Immunol2012/04/18. 19:835–841.
1048

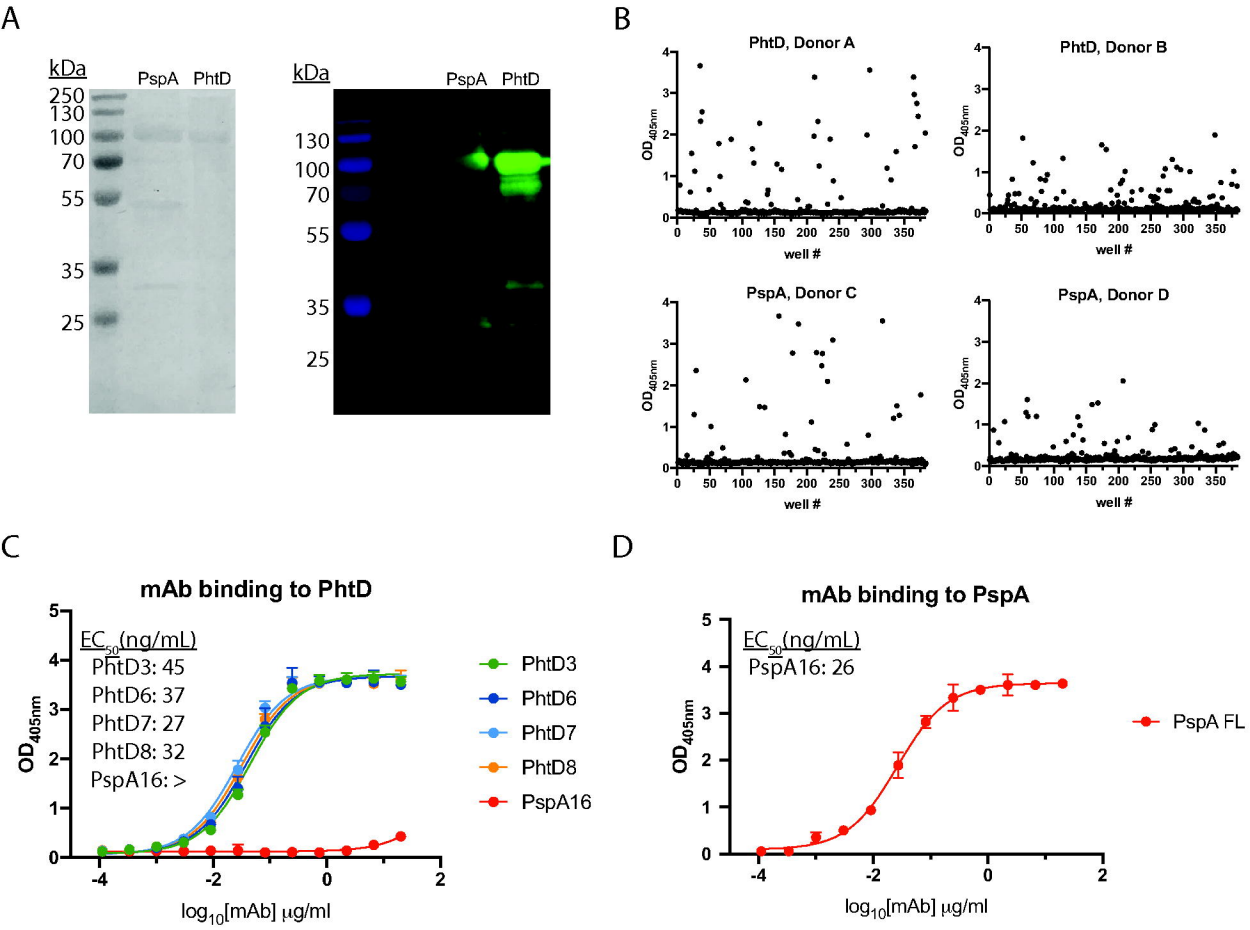

A

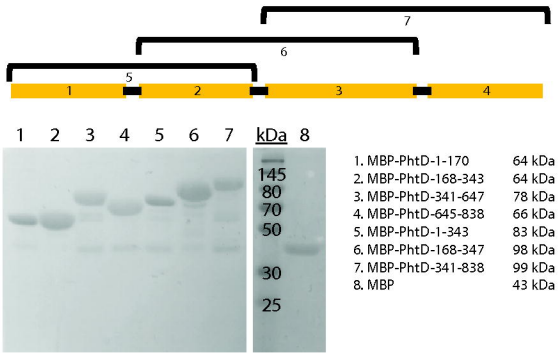

B

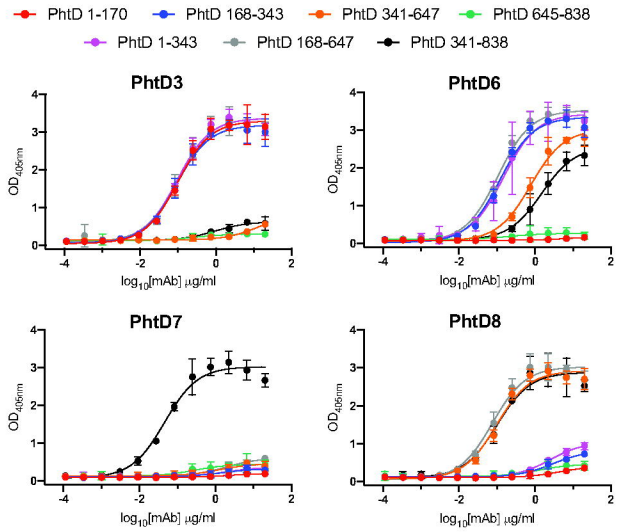

Fragment	1	2	3	4	5	6	7
Amino acids	1-170	168-343	341-647	645-838	1-343	168-647	341-838
PhtD3							
PhtD6							
PhtD7							
PhtD8							

C

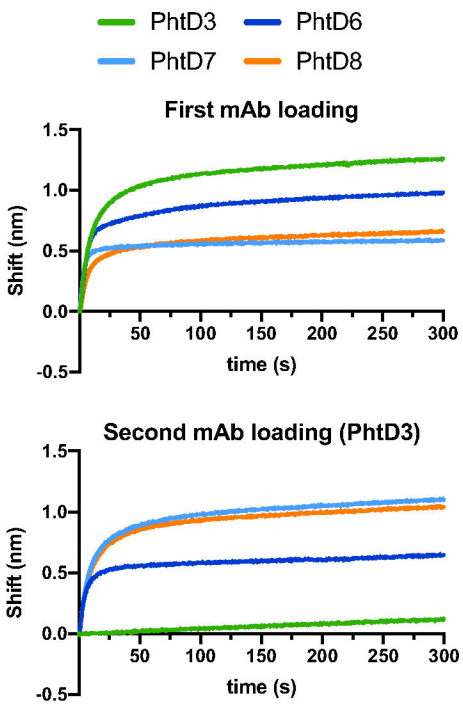

D

Second mAb

First mAb	PhtD3	PhtD6	PhtD7	PhtD8
PhtD3	9	46	80	69
PhtD6	47	12	57	66
PhtD7	81	84	18	95
PhtD8	77	72	67	27

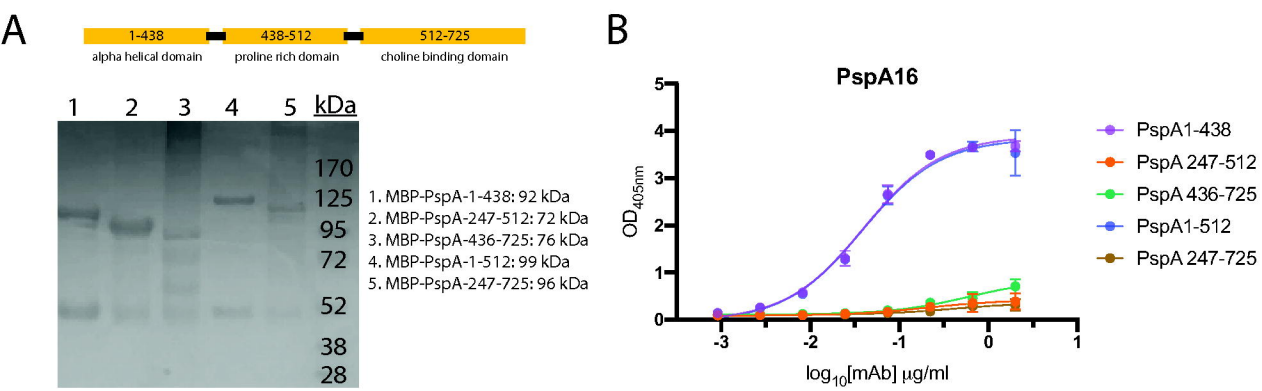

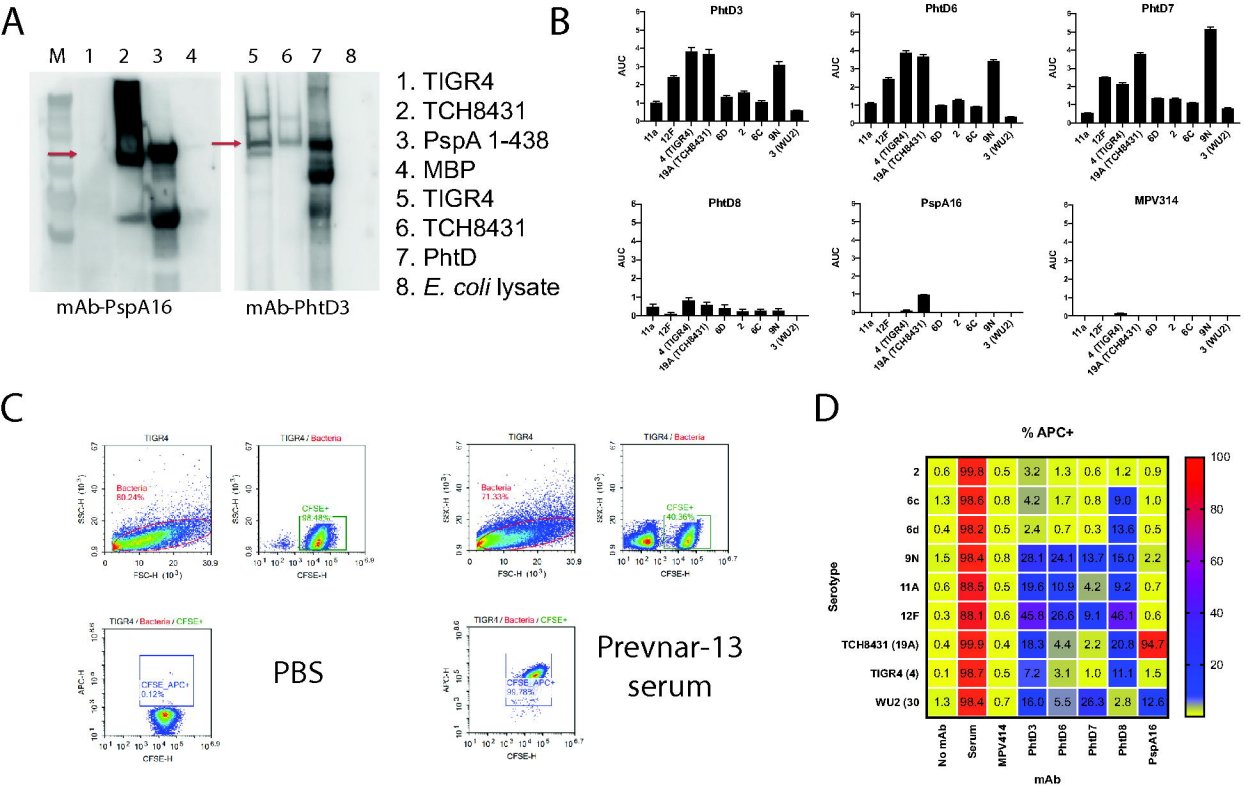

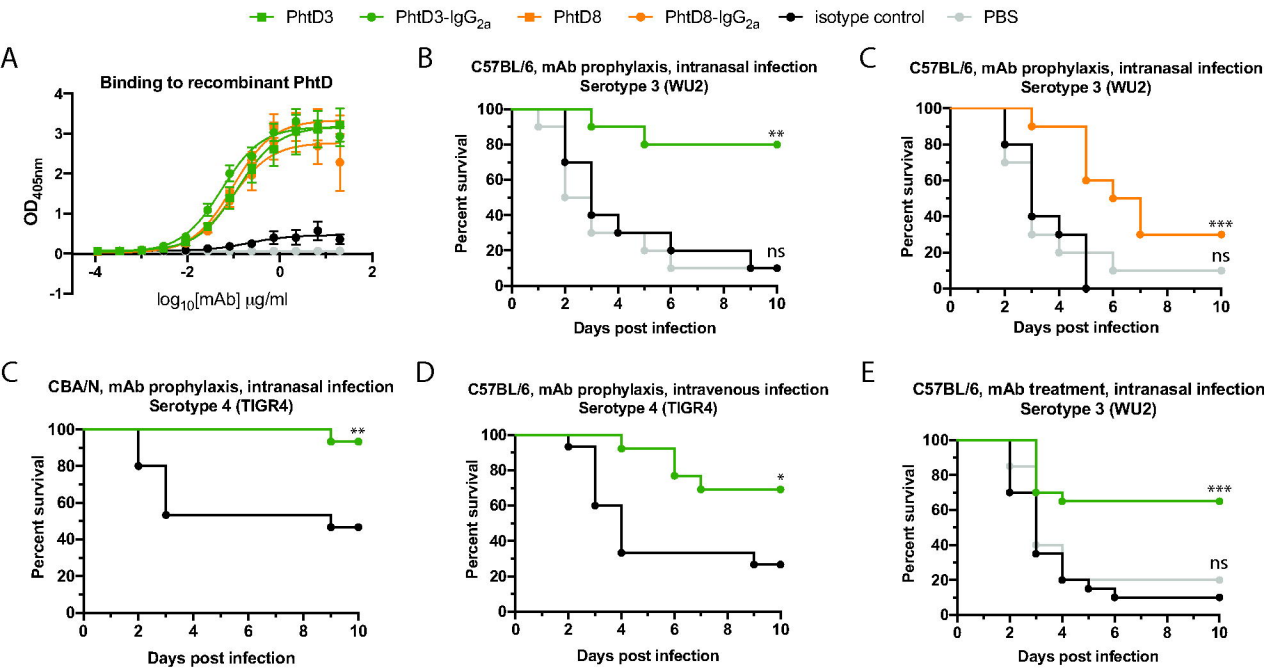

A

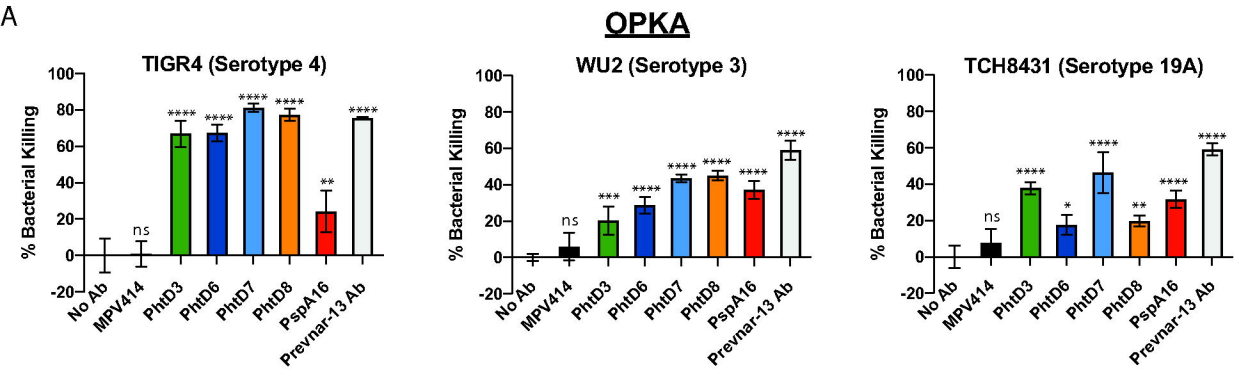

B